

Optimization in random field Ising models by quantum annealing

Matti Sarjala,¹ Viljo Petäjä,¹ and Mikko Alava¹

¹ *Helsinki University of Techn., Lab. of Physics, P.O.Box 1100, 02015 HUT, Finland*

We investigate the properties of quantum annealing applied to the random field Ising model in one, two and three dimensions. The decay rate of the residual energy, defined as the energy excess from the ground state, is found to be $e_{res} \sim \log(N_{MC})^{-\zeta}$ with ζ in the range 2...6, depending on the strength of the random field. Systems with “large clusters” are harder to optimize as measured by ζ . Our numerical results suggest that in the ordered phase $\zeta = 2$ whereas in the paramagnetic phase the annealing procedure can be tuned so that $\zeta \rightarrow 6$.

PACS numbers: 02.70.Uu, 02.70.Ss, 75.10.Nr

I. INTRODUCTION

It is desirable to have an optimization method which can be applied to as wide range of problems. An example method is the classical simulated annealing (SA). During the recent years quantum annealing (QA) has gained a lot of attention as a promising candidate for a method, with a promise of a faster convergence to the optimal configuration for a given problem. This has been partly motivated by real world realizations, demonstrated in experiments by Brooke et al. [1].

Test problems for QA can be found from many problem-specific optimization algorithms which find the exact ground state in a polynomial time, as for instance the random field Ising model or the Ising spin glass in two dimensions [2]. A convenient measure for the effectiveness of the annealing is the residual energy e_{res} which gives the energy difference between the true ground state and the configuration that is obtained in the end of the annealing process. The most important quantity is the annealing time τ , during which the temperature (transverse field in the case of quantum annealing) of the system is reduced to zero. When τ is increased the energy of the resulting configuration approaches the ground state energy.

For classical simulated annealing it has been predicted by Huse and Fisher [3] that the residual energy e_{res} decreases with the annealing time τ as

$$e_{res} \sim \log(\tau)^{-\zeta} . \quad (1)$$

For large time scales they have derived an upper limit for the decay of the residual energy in two-level systems: $\zeta \leq 2$. This result is argued to hold also for random field magnets and other disordered spin systems. The existence of a phase transition can change the value of ζ . According to Ref. [3] when a random field magnet is cooled through the phase boundary from the disordered to the ordered phase the annealing slows down to $\zeta = 1$.

In Ref. [4] Santoro et al. have studied quantum annealing in the case of a two dimensional (2d) spin glass. They have derived a theoretical estimate for the decay rate of the residual energy. Santoro et al. argued that the residual energy comes from tunnelings at (avoided) Landau-Zener (LZ) crossings. The corresponding average resid-

ual energy resulting from this process was estimated as $e_{res}(\tau) = \int_0^{\Gamma_0} d\Gamma Z(\Gamma) E_{ex}(\Gamma) \exp(\tau/\tau_c(\Gamma))$ where $Z(\Gamma)$ is the density of LZ crossings and $E_{ex}(\Gamma)$ is the corresponding average excitation energy. The term $\exp(\tau/\tau_c(\Gamma))$ gives the probability that the system tunnels during the annealing to a higher energy eigen-state due to LZ crossings, and $\tau_c(\Gamma) \sim \exp(A/\xi(\Gamma))$ where ξ is a typical wave localization length. Ref. [4] now considers the limit $\Gamma \rightarrow 0$ which is expected to dominate the annealing behavior. With the assumptions $\xi(\Gamma) \sim \Gamma^\varphi$ and $Z(\Gamma)E_{ex}(\Gamma) \sim \Gamma^\omega$ one gets $e_{res} \sim \log(\tau)^{-\zeta}$ with $\zeta = (1 + \omega)/\varphi$. With estimates $\varphi = 1/2$ and $\omega = 2$ given in Ref. [4] one gets $\zeta = 6$. The value for φ comes from a quasi-classical consideration of a particle's wave length, whereas $\omega = 2$ can be reasoned for as follows. In the limit $\Gamma \rightarrow 0$ the transverse field can be considered as a perturbation for which only the second order correction to the energy has a non-zero value. From this follows that $E_{ex} \sim \Gamma^2$. If the density of LZ crossings in the limit $\Gamma \rightarrow 0$ is assumed to be at most the density of the classical states at $\Gamma = 0$ one gets $\omega = 2$. Thus the residual energy decreases logarithmically but now with much larger exponent $\zeta \approx 6$. This implies a considerable speed-up compared to $\zeta = 2$, the upper limit of SA. It is useful to emphasize that this estimate for ζ is obtained without any problem-specific assumptions.

The numerical results of Santoro et al. [4] show that the residual energy of the 2d Edwards-Anderson spin glass converges indeed at much faster rate and to lower values with QA, compared to SA, though no empirical values of ζ were given. In addition, the performance of QA has been tested also on the traveling salesman problem [5] for which similarly to 2d spin glass it was found that QA gives a faster decay of the residual energy than SA. However, this is not generally valid for all optimization problems. Battaglia et al. [6] have found that in the case of the three-satisfiability problem quantum annealing is outperformed by simulated annealing. In small systems, it is possible to see a power law decay of the residual energy, e.g. by solving the time-dependent Schrödinger equation adiabatically [7, 8]. However, with increasing system sizes the energy gap for the Landau-Zener crossings decreases [9], which means that the probability of staying in the ground state decreases as well leading to

the logarithmic behavior discussed above.

In this paper we study the quantum annealing applied to the random field Ising model. The RFIM has the following Hamiltonian:

$$H = -J \sum_{\langle i,j \rangle} s_i s_j - \sum_i h_i s_i, \quad (2)$$

where $J > 0$ is the coupling constant, $s_i = \pm 1$ are classical spin variables and h_i is the random field at site i . One of the advantages of RFIM as a test problem is the fact that its exact ground state can be found in a polynomial time with an efficient graph algorithm from combinatorial optimization [2]. This allows us to calculate the residual energy as the difference between the true ground state and the configuration given by any annealing procedure.

Another feature of RFIM is the fact that the phase diagram depends on both dimension and the strength of disorder. The second order phase transition of the 2d Ising model is destroyed by the random fields, though residual ordering persists in finite systems [10]. Though there is thus no long range order either in one or two dimensions, systems of a finite size may have ordered ground states when the typical cluster size exceeds the system size, which is true also at zero temperature [10, 11, 12]. However, in three dimensions one has a temperature dependent critical strength of the random field $h_c(T)$ below which the system is ordered [13]. At zero temperature its value has been calculated numerically as $h_c(T=0) = 2.27$ [14].

We calculate the residual energy as a function of annealing time measured in Monte Carlo steps in one, two and three dimensions with varying strength of disorder. Our numerical results suggest that the residual energy decays logarithmically as in Eq. (1). However, the value of the exponent ζ now seems to depend on the nature of the ground state. In the ferromagnetic case $\zeta \approx 2$, whereas in the paramagnetic case $\zeta \approx 6$, if the cooling schedule is tuned well enough. To our knowledge this is the first time when empirical values for ζ are presented if not counting the simple models giving a power law decay of the residual energy [7, 8].

The structure of the rest of the paper is the following. In section II we briefly review the Suzuki-Trotter mapping which transforms a d -dimensional quantum system to a $d+1$ -dimensional classical one making the problem accessible for conventional Monte Carlo sampling. Section III is devoted to the numerical results starting with the results for the classical simulated annealing, which serve as a measuring stick when the efficiency of the quantum annealing is discussed later on. For quantum annealing we discuss numerical results in one, two and three dimensions for different random field strengths. It is also studied how the performance of QA is affected when the parameters of the $d+1$ -dimensional equivalent classical system are varied. The paper is summarized in Section IV.

II. NUMERICS

The quantum version of Eq. (2) is obtained by replacing the spin variables s_i with Pauli spin operators σ_i^z . Quantum fluctuations are tuned by changing the strength Γ of a perpendicular field term, arising from the Pauli spin operator σ_i^x .

$$H_Q = -J \sum_{\langle i,j \rangle} \sigma_i^z \sigma_j^z - \sum_i h_i \sigma_i^z - \Gamma \sum_i \sigma_i^x. \quad (3)$$

In the quantum annealing one starts with a large value of Γ so that spins in the z direction are totally uncorrelated. By decreasing Γ gradually towards zero spins fall into the ground state configuration provided that $T = 0$.

With the Suzuki-Trotter mapping [15] this d -dimensional quantum system can be represented by P coupled replicas of the classical system, Eq. (2) resulting in a $d+1$ dimensional classical problem with the following Hamiltonian:

$$H_{ST} = - \sum_{k=1}^P \left(J \sum_{\langle i,j \rangle} s_i^k s_j^k + \sum_i h_i s_i^k + J_{\perp} \sum_i s_i^k s_i^{k+1} \right), \quad (4)$$

where J_{\perp} is the Γ -dependent coupling constant between the replicas:

$$J_{\perp} = -\frac{PT}{2} \ln \tanh \frac{\Gamma}{PT}. \quad (5)$$

The resulting system has periodic boundary conditions in the extra dimension. It is convenient to set periodic boundaries also for the original classical system. The annealing of the Hamiltonian (Eq. (3)) is simulated by a standard Monte Carlo sampling of Eq. (4) at the effective temperature PT with gradually decreasing Γ .

The values of random field h_i are taken from the fixed Gaussian distribution $P_G(h_i)$ with the parameters $\langle h_i \rangle = 0$ and $\langle h_i^2 \rangle = 1$. The strength of the random field is tuned by varying the ferromagnetic coupling constant J . The residual energy e_{res} is calculated as

$$e_{res}(N_{MC}) = \langle E_{cl}(N_{MC}) \rangle_k - E_{GS}, \quad (6)$$

where $\langle E_{cl} \rangle_k$ is the average energy of all replicas and E_{GS} is the ground state energy. The GS energy and configuration are computed for each sample, as noted in the introduction, by using a combinatorial optimization algorithm. Both $\langle E_{cl}(N_{MC}) \rangle_k$ and E_{GS} from the definition in Eq. (6) are normalized per spin.

III. RESULTS

A. Classical simulated annealing

First, we briefly present numerical results for classical simulated annealing, which are then later utilized

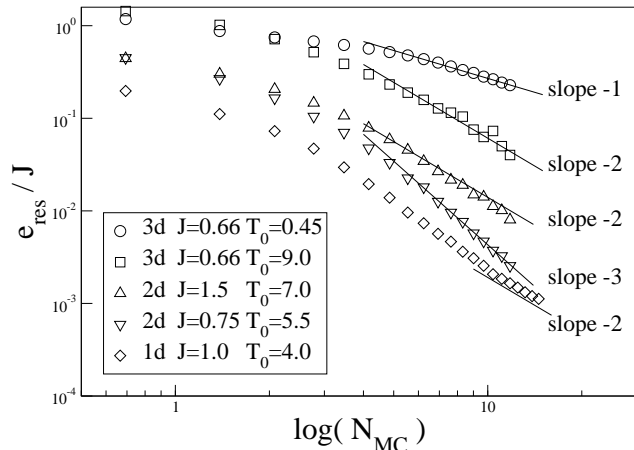


FIG. 1: A doubly logarithmic plot of residual energies in classical simulated annealing. $L = 32$ in 3d, $L = 256$, in 2d and $L = 10^4$ in 1d with different coupling constants J and initial temperatures T_0 . The straight lines are guides for the eye.

in a comparison with quantum annealing. Since the differences between various trial annealing schedules in the case of SA turned out to be rather small we show in Fig. 1 only the data that corresponds to a linear cooling schedule. In one and two dimensions we find the expected logarithmic decrease of the residual energy ($e_{res} \sim \log(N_{MC})^{-\zeta}$) with $\zeta = 2..3$. According to Ref. [3] $\zeta = 2$ is an upper limit, and hence it is expected that asymptotically $\zeta \rightarrow 2$.

In 3d in the ordered phase, for $J > J_c \approx 0.44$ [14], one can observe the slowing effect of the phase transition on the cooling efficiency in agreement with the theoretically predicted $\zeta = 1$ [3]. This is clearly visible for the case where the annealing is started at low temperature (ovals). When the starting temperature is well above T_c the system stays in the paramagnetic phase during most of the simulation time resulting in $\zeta = 2$. With increasing number of Monte Carlo steps the system is expected to spend more annealing steps in the ferromagnetic phase and hence to experience the slowing of the annealing rate to $\zeta = 1$.

B. Quantum annealing: preliminaries

A priori it is naturally not clear which is the best way to reduce the value of Γ . We have tested the three following annealing schedules:

$$\Gamma_{\text{Lin}}(N) = \Gamma_0 \left(1 - \frac{N}{N_{MC}}\right), \quad (7)$$

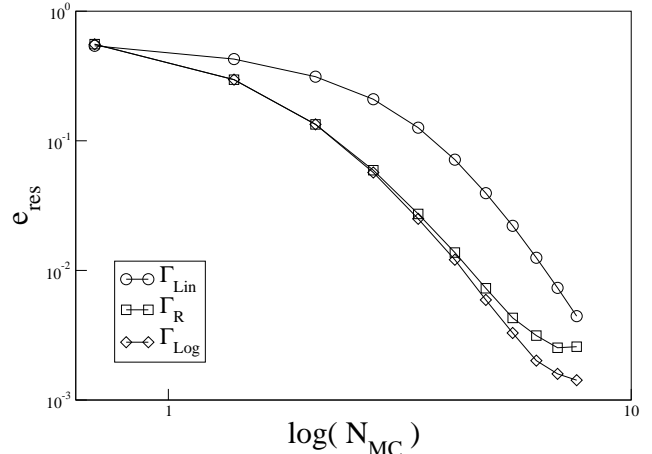


FIG. 2: A doubly logarithmic plot of residual energies in 1d corresponding to different quantum annealing schedules Eqs. (7)-(9).

$$\Gamma_R(N) = \Gamma_0 / \left(1 + R \frac{N}{N_{MC}}\right), \quad R = \frac{\Gamma_0}{\Gamma_f} - 1, \quad (8)$$

$$\Gamma_{\text{Log}}(N) = -\log \left\{ \tanh \left[\text{atanh}(e^{-\Gamma_0}) - \frac{N}{N_{MC}} (\text{atanh}(e^{-\Gamma_0}) - \text{atanh}(e^{-\Gamma_f})) \right] \right\}. \quad (9)$$

The residual energies corresponding to the different schedules (Eqs. (7)-(9)) for 1d systems of 10^4 spins (averaged over more than 10 samples each) are shown in Fig. 2. With the used set of parameters ($J = 1, PT = 4, P = 128, \Gamma_0 = 8, \Gamma_f = 10^{-6}$) the residual energies seem to decay with the same slope for all annealing schedules. However, the logarithmic schedule (Eq. (9)) gives the lowest residual energy and hence we restrict ourselves to it throughout the rest of the paper. The choice of Γ_0 does not alter the results as far as it is chosen large enough in order to ensure that there are no correlations in the starting configuration. We flip only one spin at a time. We tested also the use of the global flips where one attempts to flip all replicas of a given spin. It turned out that the single flip strategy is more effective.

The typical evolution of the quantum annealing in 1d is illustrated with snap-shots of the spin configurations in Fig. 3. The 256 replicas of the original classical system of size $L = 256$ lie in the horizontal direction. Black pixels represent spins which match with the orientation in the ground state configuration, while white pixels correspond to incorrectly aligned spins. Note how the effectively classical system is strongly correlated along the Trotter direction.

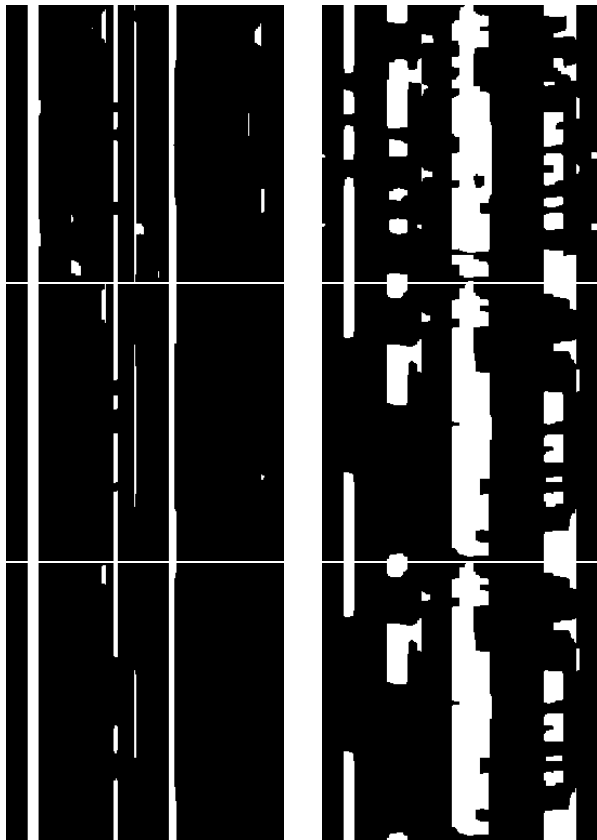


FIG. 3: Snapshots of the spin configurations in the process of the annealing after (from top to bottom) $1/3N_{MC}$, $2/3N_{MC}$ and N_{MC} (final) Monte Carlo iterations. Black color denotes correctly aligned spins with respect to the ground state. Right: $J = 2.0$, left: $J = 4.0$ ($L = 256$, $P = 256$, $PT = 2$, $\Gamma_0 = 40$, logarithmic annealing scheme).

C. Quantum annealing: one dimension

The Suzuki-Trotter mapping is exact only in the limit $PT \rightarrow \infty$. This means that the quantum nature of annealing should not be seen when the value of PT is too small. On the other hand in order to find the ground state of the system the temperature T needs to be taken to zero. In the ideal case one should have $PT \rightarrow \infty$ and $T = 0$, simultaneously, which is impossible in practice.

With $P = 1$ one simply performs Metropolis dynamics, and as P is increased the annealing should become more efficient. This is demonstrated in Fig. 4 for 1d systems of 10^4 spins. The effective temperature is kept constant $PT = 4$ while the number of the Trotter replicas P is varied. The results are averaged over 10 realizations of disorder, each.

When P is increased sufficiently ($P > 32$) one can observe a region where the annealing rate of QA is considerably higher compared to SA. With increasing P this region grows and we expect that this is the asymptotic behavior for $P \rightarrow \infty$. Since the Suzuki-Trotter mapping is exact in this limit, one can assume that this region

reflects the properties of quantum annealing with a finite, non-zero quench rate. For finite values of P the system falls out of this quantum annealing regime to the classical Metropolis behavior as N_{MC} is increased. In the classical regime the system is fully correlated in the Trotter direction and the annealing process cannot anymore take an advantage of the extra, non-classical dimension. This means that in order to maintain a fast annealing rate for large values of N_{MC} larger P values are needed as well, as was also observed in Ref. [16]. Due to the finite simulation temperature the residual energy finally saturates to some non-zero value.

As indicated in Fig. 5 the decay rate of e_{res} depends on the actual value of the coupling constant J . The case with $J = 0$ and $\langle h^2 \rangle = 1$ is a problem of L^d independent spins for which the results depend on the used annealing schedule [17]. For the logarithmic and rational schedules (Eq. (9)) we find a polynomial decay of the residual energy $e_{res} \sim (N_{MC})^{-\tilde{\zeta}}$ with $\tilde{\zeta} \approx 2$ whereas in the case of the linear annealing schedule $\tilde{\zeta} \approx 1$. For $J > 0$ the quantum annealing goes over to the logarithmic regime $e_{res} \sim \log(N_{MC})^{-\zeta}$. The numerical values of ζ roughly agrees with the estimate $\zeta_{max} = 6$ given by Santoro et al. [4]. As J grows, and hence the cluster sizes of the ground state, the annealing efficiency seems to diminish. When no random field is applied the dynamics of the quantum annealing in the limit $\Gamma \rightarrow 0$ for $P \gg L$ corresponds to a case of a strongly anisotropic Ising model. In Ref. [18] Ferreira et al. have studied the two dimensional anisotropic Ising system with $J_x \gg k_B T \gg J_y$. They found that in the large time limit the width of the interfaces perpendicular to x -direction saturates to some finite value. We have verified numerically that in same limit the quantum annealing ends up in a situation where the residual energy comes from rough, fluctuating boundaries, positioned perpendicular to the Trotter direction.

The scale of the energy barriers is determined by the value of J . Hence, when J is increased one needs larger PT to overcome the barriers. The data in Fig. 6 shows how the annealing rate grows as PT is increased. The value of PT has a two-fold effect. As indicated in Fig. 6 large values of PT are desirable in order to minimize the error in the Suzuki-Trotter mapping and hence to be able to observe the true quantum annealing behavior. On the other hand the PT determines the growth rate of J_{\perp} (see Eq. 5). As PT increases one needs larger a N_{MC} in order to keep the same annealing rate and hence to reach an equally low value of e_{res} .

D. Quantum annealing: 2d and 3d

In two dimensions we consider systems with sizes only up to 128×128 in order to be able to consider P up to 1024. For low values of J , where the size of the clusters is well below the system size, the QA performs similarly to the one dimensional case giving $\zeta \approx 6$ for $J = 0.33$ (see Fig. 7). With J also the cluster sizes of the ground state

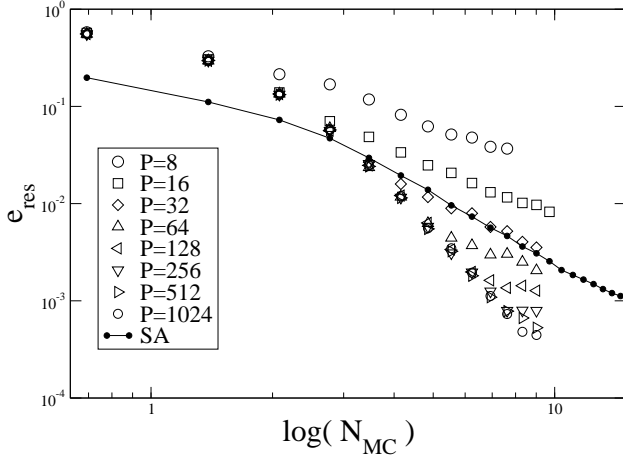


FIG. 4: A doubly logarithmic plot of residual energies in 1d with $J = 1, L = 10^4, PT = 4, P = 8 \dots 1024$. For comparison we also show the data corresponding to the classical simulated annealing (SA). In order to compare the used Monte Carlo time, in the case of QA N_{MC} has to be multiplied with the number of replicas P .

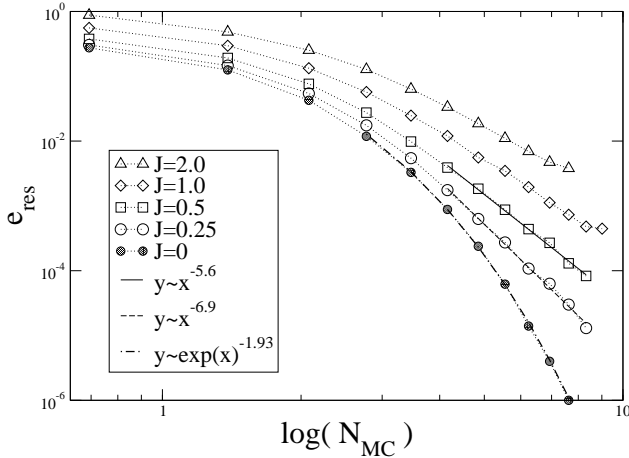


FIG. 5: A doubly logarithmic plot of 1d residual energies, $L = 10^4, PT = 4$. The $J = 0$ case is a problem of L^d independent spins for which $e_{res} \sim (N_{MC})^{-\zeta}$ with $\zeta \approx 2$. For $J > 0$ e_{res} seems to decay logarithmically. With increasing J the RFIM becomes more difficult to anneal.

grow reaching the system size (128×128) approximately at $J = 1.5$. From Fig. 7 one can see that for $J \gtrsim 1$ one has $\zeta = 2$. Whereas in the case of one dimensional systems with extremely weak disorder the value of ζ could be raised by increasing the effective temperature PT this seems not to work in two dimensions. This suggests that there is a fundamental difference in the performance of

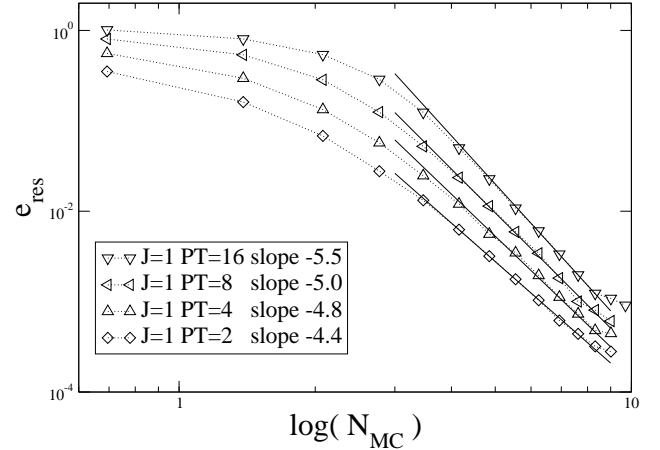


FIG. 6: A doubly logarithmic plot of residual energies in 1d with $L = 10^4, J = 1$. The annealing rate increases with PT at the cost of growing amplitude (prefactor).

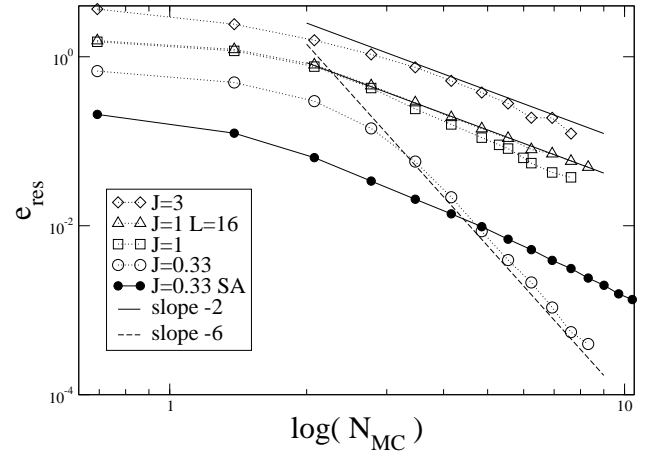


FIG. 7: A doubly logarithmic plot of residual energies in 2d, $PT = 12, L = 128$, and one data set corresponding to $L = 16$. The straight lines are guides for the eye. For $J \gtrsim 1$ the residual energy decays with $\zeta \approx 2$. With growing J no further decrease of ζ is observed. For comparison we also show the results for classical simulated annealing (SA).

QA depending whether the system has a disordered or ordered ground state. This conclusion is supported by the observation that with $J = 1$ for a larger system ($L = 128$, squares in Fig. 7) one gets lower residual energies compared to a smaller system ($L = 16$, triangles in Fig. 7) that already has an ferromagnetically ordered ground state.

As it was already evident in the 2d case also the results for 3d RFIM show that QA is sensible to the ordering of

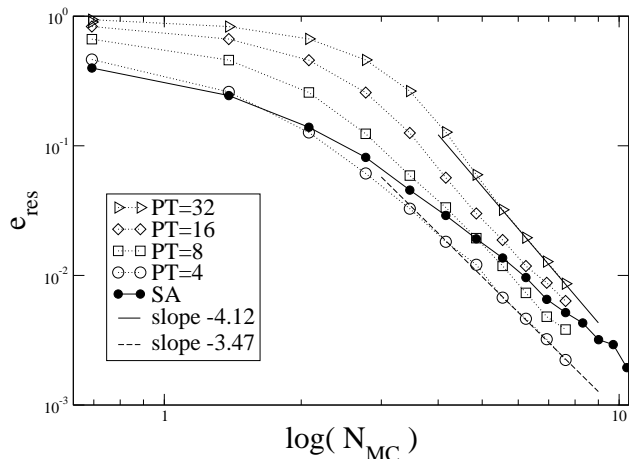


FIG. 8: A doubly logarithmic plot of residual energies in 3d, $L = 24$, $J = 0.33$. With increasing PT the effective ζ is growing. For comparison we also show the results for classical simulated annealing (SA).

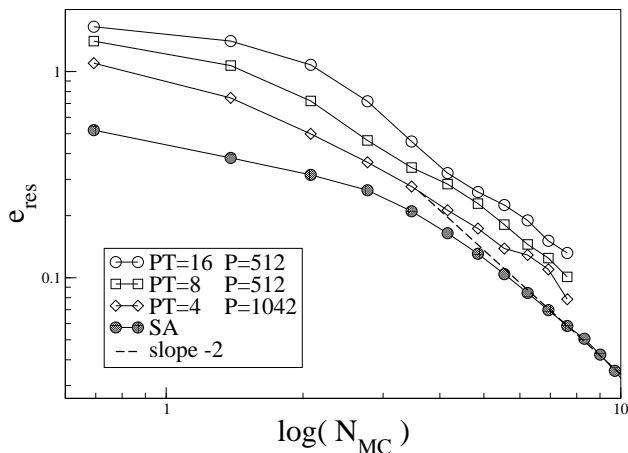


FIG. 9: A doubly logarithmic plot of residual energies in 3d, $L = 24$, $J = 0.66$. The decay rate of e_{res} does not vary with PT , $\zeta \approx 2$. For comparison we also show the results for classical simulated annealing (SA).

the underlying system. For low values of J ($J < J_c \approx 0.44$ [14]) where the system is in the paramagnetic phase also at $T = 0$ we find the same behavior as in one and two dimensions (Fig. 8): QA is faster than SA and ζ can be tuned towards 6 by increasing PT . Fig. 9 shows the data corresponding to $J = 0.66$. For the range of parameters that have been used we find that $\zeta \approx 2$, as in 2d, for a system with an ordered ground state.

IV. SUMMARY

We have studied numerically quantum annealing in the random field Ising model and compared our results with classical simulated annealing. When the system is in the paramagnetic phase we find that asymptotically QA provides a better decay rate of the residual energy with ζ up to 6 in agreement with the Landau-Zener picture based scaling argument presented by Santoro et al. [4].

We expect that the asymptotic performance of QA in one and two dimensions does not change by varying the coupling constant J or the magnetic field strength h . With growing cluster sizes in the GS one needs increasingly larger values of PT and P for which the fast annealing rate with $\zeta \approx 6$ could be observed. The requirement of large values of P in the case of weak random field makes QA from the practical point of view slower compared to SA. Note the starting point however: that the RFIM GS can be found effectively with combinatorial optimization.

In 3d we have presented evidence that the performance of QA depends on whether the system is in the paramagnetic or ordered phase. Thus, the situation is actually analogous to the behavior of the SA. In the paramagnetic phase we find the similar behavior as in one and two dimensions. In the ordered phase we observe a much slower decay of e_{res} with $\zeta \approx 2$, so that in fact QA is slower than SA with a starting temperature $T_0 > T_c$.

We conclude with the general observation that the better efficiency of QA is most clear when the ground state consists of small clusters, i.e. the correlation length of the ground state is short compared to the number of the Trotter replicas. Such benefits vanish with an increasing correlation length, of the ground state configuration.

[1] J. Brooke, T. F. Rosenbaum, G. Aeppli, Nature, **413**, 610 (2001); J. Brooke, T. F. Rosenbaum, G. Aeppli, Science, **284**, 779 (1999).
 [2] M. Alava, P. Duxbury, C. Moukarzel, and H. Rieger, in Phase transitions and Critical phenomena, edited by C. Domb and J.L Lebowitz Academic Press, San Diego, vol 18 (2001).
 [3] D. A. Huse, D. S. Fisher, Phys. Rev. Lett., **57**, 2203

(1986)
 [4] G. E. Santoro, R. Martoňák, E. Tosatti, R. Car, Science **295**, 2427 (2002).
 [5] R. Martoňák, G. E. Santoro, E. Tosatti, Phys. Rev. E **70**, 057701 (2004).
 [6] D. A. Battaglia, G. E. Santoro, E. Tosatti, Phys. Rev. B **72**, 014303 (2005).
 [7] S. Suzuki and M. Okada, J. Phys. Soc. Jpn. **74**, 1649

- (2005); see also S. Suzuki and M. Okada in “Quantum Annealing and Related Optimization Methods”, Eds. A. Das and B. K. Chakrabarti, Lect. Notes in Phys., Vol. 679, Springer, Heidelberg (2005), pp 207-283.
- [8] L. Stella, G. E. Santoro, and E. Tosatti, Phys. Rev. E **71**, 066707 (2005).
- [9] J. Dziarmaga, Phys. Rev. Lett. **95**, 245701 (2005).
- [10] E. T. Seppälä, V. Petäjä, and M. J. Alava, Phys. Rev. E **58**, R5217 (1998); E. T. Seppälä and M.J. Alava, Phys. Rev. E **63**, 066109 (2001).
- [11] G. Schröder, T. Knetter, M. J. Alava, and H. Rieger, Euro. Phys. J. B **24**, 101 (2001).
- [12] M. Aizenman and J. Wehr, Phys. Rev. Lett. **62**, 2503 (1989).
- [13] J. Z. Imbrie, Phys Rev. Lett. **53**, 1747 (1984); J. Bricomont and A. KUPIAINEN, Phys. Rev. Lett. **59**, 1829 (1987).
- [14] A. A. Middleton and D. S. Fisher, Phys. Rev. B **65**, 134411 (2002).
- [15] M. Suzuki, Prog. Theor. Phys. **56**, 1454 (1976).
- [16] R. Martoňák, G. E. Santoro, E. Tosatti, Phys. Rev. B **66** 094293 (2002).
- [17] T. Kadowaki and H. Nishimori, Phys. Rev. E **58**, 5355 (1998).
- [18] A. L. C. Ferreira, S. K. Mendiratta and E. S. Lage, J. Phys. A: Math. Gen. **22**, L431 (1989).